

# Adaptable Lipid Matrix Promotes Protein–Protein Association in Membranes

Andrey S. Kuznetsov,<sup>†</sup> Anton A. Polyansky,<sup>†,‡</sup> Markus Fleck,<sup>‡</sup> Pavel E. Volynsky,<sup>†</sup> and Roman G. Efremov<sup>\*,†,§</sup>

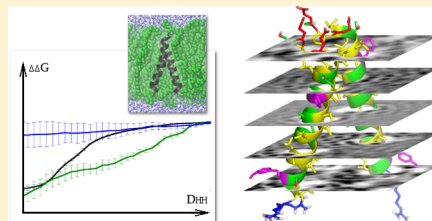
<sup>†</sup>M. M. Shemyakin and Yu. A. Ovchinnikov Institute of Bioorganic Chemistry, Russian Academy of Sciences, Miklukho-Maklaya Str., 16/10, Moscow 117997, Russia

<sup>‡</sup>Department of Structural and Computational Biology, Max F. Perutz Laboratories, University of Vienna, Campus Vienna Biocenter 5, Vienna AT-1030, Austria

<sup>§</sup>Higher School of Economics, Myasnitskaya Str., 20, Moscow 101000, Russia

## Supporting Information

**ABSTRACT:** The cell membrane is “stuffed” with proteins, whose transmembrane (TM) helical domains spontaneously associate to form functionally active complexes. For a number of membrane receptors, a modulation of TM domains’ oligomerization has been shown to contribute to the development of severe pathological states, thus calling for detailed studies of the atomistic aspects of the process. Despite considerable progress achieved so far, several crucial questions still remain: How do the helices recognize each other in the membrane? What is the driving force of their association? Here, we assess the dimerization free energy of TM helices along with a careful consideration of the interplay between the structure and dynamics of protein and lipids using atomistic molecular dynamics simulations in the hydrated lipid bilayer for three different model systems – TM fragments of glycophorin A, polyalanine and polylysine peptides. We observe that the membrane driven association of TM helices exhibits a prominent entropic character, which depends on the peptide sequence. Thus, a single TM peptide of a given composition induces strong and characteristic perturbations in the hydrophobic core of the bilayer, which may facilitate the initial “communication” between TM helices even at the distances of 20–30 Å. Upon tight helix–helix association, the immobilized lipids accommodate near the peripheral surfaces of the dimer, thus disturbing the packing of the surrounding. The dimerization free energy of the modeled peptides corresponds to the strength of their interactions with lipids inside the membrane being the lowest for glycophorin A and similarly higher for both homopolymers. We propose that the ability to accommodate lipid tails determines the dimerization strength of TM peptides and that the lipid matrix directly governs their association.



## INTRODUCTION

Integral membrane proteins enable communication between extra- and intracellular spaces and contain plasma membrane embedded domains, which are usually comprised of  $\alpha$ -helical segments. Most often, these transmembrane (TM) helices do not stay isolated in the lipid environment but tend to form interacting pairs (hairpins, noncovalent dimers) or more complex aggregates (helical bundles, noncovalent oligomers) instead. Such an assembly and rearrangement of TM domains’ conformations are a prerequisite for switching a protein to its active state. A malfunction of the helix packing leads to severe diseases, like myeloma, urinary bladder cancer, or other.<sup>1,2</sup> This creates a strong incentive for developing a better understanding of the molecular details of such processes in order to regulate the biological functioning of these systems in a goal-oriented manner. Although during the last decades a certain progress has been achieved in our understanding of membrane proteins’ folding energetics as well as cotranslational assembly of multispan membrane proteins directed by the translocation machinery<sup>3–6</sup>, the intermolecular self-association of TM  $\alpha$ -

helices of two or more proteins is much less understood. Particularly, a number of crucial questions need to be addressed: (i) How do the helices recognize and/or find each other in such a heterogeneous medium as the cell membrane? (ii) What are the main factors determining the spontaneous binding between them? (iii) What defines the strength and specificity of the association? Aside from a great fundamental importance, addressing these issues opens extremely intriguing perspectives in the design of TM peptides or other classes of molecules with predefined ability to interact with a given TM helix – a putative pharmacological target – and modulate the function of its host protein.

Taking into account the complexity of the protein–membrane systems, current efforts are focused on experimental and computational studies of their simplest models – two TM helices in hydrated lipid bilayers. Such models do not represent just a toy example, but they are also relevant for the

Received: March 3, 2015



understanding of the function of single-pass (bitopic) membrane proteins. Among them, the receptor tyrosine kinases (RTK) regulating the cell division and growth are the ones of great biomedical interest. Their TM domains have been shown to play a crucial role in the dimerization and activation of these receptors, which are mainly implicated in the modulation of mutual orientation of intracellular kinase domains and the subsequent control of self-phosphorylation.<sup>7,8</sup> Since the model of interacting membrane-spanning  $\alpha$ -helices is relevant for understanding the assembly of the most membrane proteins and can be directly applied to RTKs, the process of TM dimers formation has been widely studied. The latter includes considerable progress in the determination of spatial (3D) structures of TM helical dimers experimentally using solution NMR in different membrane mimetics<sup>9–14</sup> and via computational modeling.<sup>15–23</sup> The analysis of experimental/predicted structures yields in a simplistic explanation of the potential association between helices by the presence of particular dimerization patterns or motifs<sup>24–26</sup> in their sequences. Namely, this is a well-known “glycophorin-like” ( $GG_4$ ) motif: GXXXG, where “G” and “X” correspond to amino acids with a small side-chain (Gly, Ala, rarely – Ser) and any residue, respectively. The presence of one or several of  $GG_4$  motifs within TM sequences is usually attributed to potential dimerization via these regions. However, motifs themselves neither represent a necessary and sufficient criterion of a dimer formation nor predefine the dimerization interface. In a number of experimentally obtained dimer models, helices utilize other sequence regions for packing, even if  $GG_4$  motifs are present, or select a specific one among the several available  $GG_4$  motifs.<sup>13,27</sup>

The strength of the association between TM helices can be estimated using both experimental and computational techniques in terms of the free energy of dimerization ( $\Delta G$ ).<sup>23,28–32</sup> Although direct contacts between monomers are obviously important (e.g., van der Waals packing and hydrogen bonding<sup>33,34</sup>), the results of the dimerization free energy estimations for TM dimers suggest that the membrane can also contribute significantly to the association of TM helices. The lipid composition of a bilayer and hence the physicochemical properties related to it, such as the charge of the lipid polar head, the hydrophobic thickness and the lipid acyl chain order (phase) have been shown to modulate the strength of interactions between TM helices.<sup>18,19,35–39</sup> The latter is also true for the cholesterol content of model membranes.<sup>35,40</sup> The role of the membrane is particularly important in the context of the existence of multiple possible conformational states of TM helical dimers. As we have shown in our recent studies, changing the lipid environment leads to a preferential stabilization of certain dimeric conformations from the ensemble via a prominent increase in the absolute free energy value for the states with an optimal crossing angle and interface between the helices.<sup>18,19</sup> Despite being typical of any signaling systems, this important aspect has been rarely discussed so far. Apart from creating a suitable environment for helix–helix interactions, lipids have also been found to possess specific binding sites in the TM domains of multipass integral membrane proteins,<sup>41–44</sup> and such sites can potentially affect the helix association, even in the simplest dimer case.

Altogether, the self-association of TM helices is governed by the interplay between the physicochemical properties of the two major players – the peptide and the membrane. The contribution of the former is sequence-dependent and includes

a combination of the following factors and their dynamic characteristics: the exact spatial distribution of hydrophobic/hydrophilic and geometric surface properties over the peptide length and the interactions of peptide with the lipid/water surrounding. Membrane contribution also depends on the lipid composition, which determines the geometry of the bilayer (thickness, packing density, domain structure), its dynamic organization (ordering of acyl chains, distribution and fluctuation of free volume, dynamics of water, etc.), and the microscopic details of peptide-membrane interactions. The particular role of the medium can be also emphasized by the fact that calculated potential of the mean force (PMF) profiles for protein–protein interaction within a dimer usually reaches zero already at distances about 20 Å where no direct protein–protein interactions exist (see e.g. ref 18). Hereinafter, the term “interhelical distance” denotes the distance between their centers of mass. What drives the association of the helices if they do not initially “see” each other? Importantly, the dimer assembly should be rather robust and precise to provide a naturally occurring functionality of the dimer. We should emphasize that the lipid membrane possesses highly heterogeneous organization both laterally and vertically. The former one is related to in-plane lipid clusterization,<sup>45,46</sup> while the latter assumes the existence of different bilayer regions along the normal, such as the heterogeneous water–lipid interface and the hydrophobic core, where lipid tails form a relatively homogeneous yet highly dynamic matrix. We speculate that communication between TM helices is ensured by this lipid matrix, which represents a medium flexible and sensible enough for an efficient discrimination between different inclusions and broadcasting interactions between them.

Here, in order to get an atomistic picture of how the membrane promotes the dimerization of membrane-spanning peptides, we use all-atom molecular dynamics (MD) simulations for three model systems – TM helix pairs, which potentially form strong, medium, and weak dimers. The peptides are immersed into the hydrated lipid bilayer and placed at different distances – from a tight complex to monomeric states. The focus is placed on the sensitivity of helix–helix binding to the properties of surrounding lipids and the amino acid sequence of the peptides. A special emphasis is done on the atomic-scale structural and dynamic parameters of lipids with and without immersed TM helices. Also, we check whether there is a correlation between this data and the strength of helix–helix interactions. Our modeling framework provides direct access to the system’s thermodynamics and ensures an exhaustive monitoring of the structural and dynamic behavior of lipids including their conformational entropy.

## METHODS

**Model Peptides.** We apply the same simulation protocols for three different peptides: (i) TM segment of a real protein, which has been shown to form strong dimers in artificial and cell membranes – glycophorin A (GpA); (ii) an nonpolar peptide composed of alanine residues (PolyALA) with a rather smooth molecular surface – due to the small size of Ala side chains and their uniform composition; (iii) a prominently hydrophobic peptide composed of leucine residues (PolyLEU) – being uniformly distributed, long branched side chains of Leu create a regular large-scale roughness on the peptide’s surface. In order to simplify the peptide-membrane systems, we neglect the role of the exact lipid composition: all MD simulations are carried out in the same lipid environment – hydrated

palmitoyloleylphosphatidylcholine (POPC) bilayer. To exclude the effects of polar termini, we take juxtapamembrane parts of the peptides identical to that in GpA (**Table 1**).

**Table 1.** Amino Acid Sequences of the Model Peptides<sup>a</sup>

name	sequence
GpA	<sup>69</sup> SEPEITLIIFGVGMAGVIGTILLISYGIRR <sup>97</sup>
PolyALA	SEPEAAAAAA <sub>n</sub> AGIRR
PolyLEU	SEPELLL <sub>n</sub> LLGIRR

<sup>a</sup>Residue numbering corresponds to that in human glycophorin A.

All-atom initial structures of monomers were built in an ideal  $\alpha$ -helical conformation using the PyMOL program (The PyMOL Molecular Graphics System, Version 1.7.2.1 Schrödinger, LLC). Arg and Glu residues, N- and C- termini were taken in charged form. The dimeric conformations for all three TM fragments were constructed using the same spatial template – the NMR structure of the GpA dimer.<sup>47</sup>

**Molecular Dynamics (MD) Simulations.** All MD simulations were performed using the GROMACS 4.5.6 package and the 43a2 parameter set from the GROMOS96 force field.<sup>48</sup> Simulations were carried out using an integration step of 2 fs and imposed 3D periodic boundary conditions. A twin-range (10/12 Å) spherical cutoff function was used to truncate van der Waals interactions. Electrostatic interactions were treated using the particle-mesh Ewald summation (real space cutoff 10 and 1.2 Å grid with fourth-order spline interpolation). MD simulations were carried out in an

isothermal–isobaric (NPT) ensemble with a semi-isotropic pressure of 1 bar and a constant temperature of 315 K. The pressure and temperature were controlled using a V-rescale thermostat<sup>49</sup> and a Berendsen barostat<sup>50</sup> with 1.0 and 0.1 ps relaxation parameters, respectively, and a compressibility of  $4.5 \times 10^{-5}$  bar<sup>-1</sup> for the barostat. Protein, lipids, and water molecules were coupled separately.

The initial configurations of the simulated systems were obtained by inserting the peptide monomer or dimer into a pre-equilibrated lipid bilayer comprised of 128 POPC molecules using the *genbox* utility from the GROMACS package. The latter procedure leads to the removal of a number of lipid molecules (10–20) to form an appropriate pore. Water molecules were added to the simulation box, and waters placed in the bilayer interior were removed from the system. The systems, thus prepared, were equilibrated by energy relaxation via 50000 iterations of the steepest descent minimization followed by heating from 5 to 315 K during a 50 ps MD run and a 50 ns MD run at 315 K with fixed positions of the peptide atoms to compensate for the bilayer distortion. Finally, three independent production MD runs of 210 ns were carried out for each system, including monomers, dimers in different states, and the pure POPC bilayer used as a reference system.

**Calculation of the Free Energy Profiles.** Potential of mean force (PMF) profiles for each dimer were calculated as a function of interhelical distance. The distance between the centers of mass was considered as a reaction coordinate  $r$ . In total, 32 windows were taken for the umbrella sampling with  $r$  varying from 7.0 to 22.5 Å. This results in about 10  $\mu$ s of the total MD time. A set of reference structures was obtained by

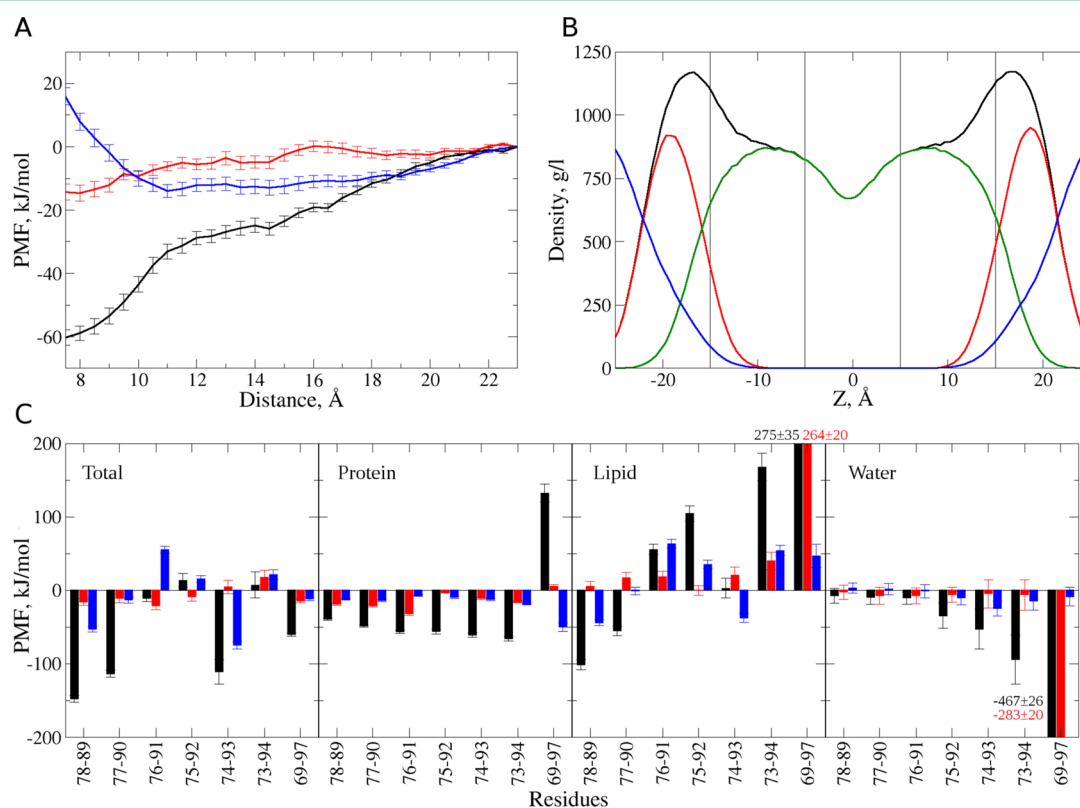


**Figure 1.** Potential of mean force (PMF) profiles for GpA (black), PolyALA (red), and PolyLEU (blue) peptides (A). The average density profiles for water (blue) and lipids as a function of the distance from the bilayer center (Z): total lipid density (black), polar heads (red), and acyl chains (green) (B). Energy contributions of different fragments of peptide into total free energy (“Total”) and its protein–protein (“Protein”), protein–lipid (“Lipid”), and protein–water (“Water”) components for GpA (black), PolyALA (red), and PolyLEU (blue) peptides in the POPC bilayer (C).

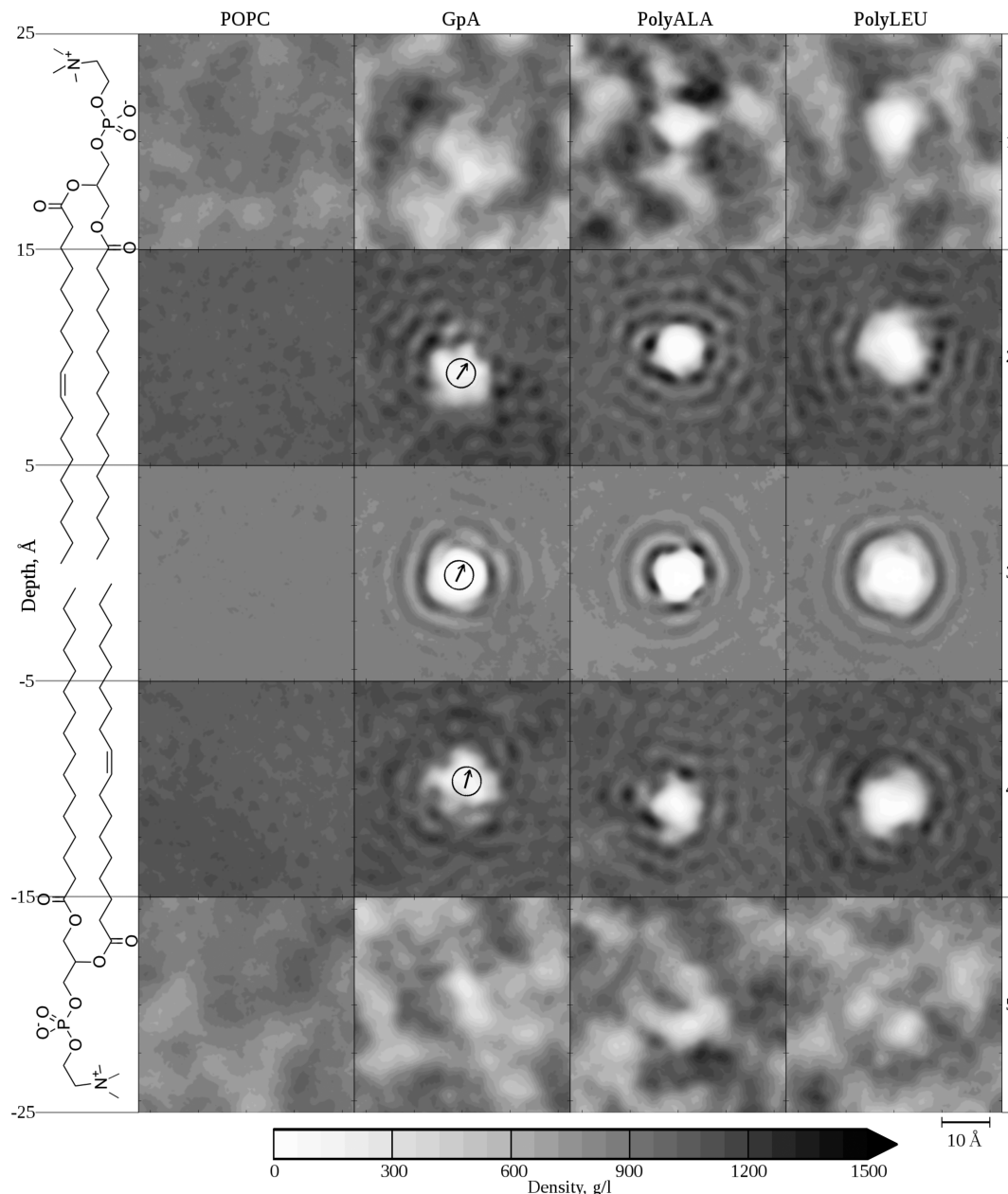


**Figure 2.** In-plane distributions of the average lipid density for a number of the bilayer slices carved along the membrane normal for the “pure” POPC bilayer and bilayers containing peptide monomers: GpA, PolyALA, and PolyLEU. Darker areas correspond to higher density. Schematic representation of the POPC molecule is shown on the left. Each slice is 10 Å wide. The white pore corresponds to the inserted peptide. Circle shows average position of GpA peptide (only on slices 2–4) with an arrow pointing to its interface of dimerization (residues G79, G83, T87). N-terminal of the peptide is on the top, and C-terminal corresponds to the bottom slice. Detailed view of central slices with marked positions of amino acids is shown in Figure S2.

translating monomers in the membrane plane along the line connecting their centers of mass. The initial structure for each window was generated using 50 ns MD equilibration (with the same protocol as mentioned before), where positions of the monomers were fitted to the reference structure. The 50 ns production MD runs were carried out in each window with a harmonic force constant of  $10 \text{ kJ mol}^{-1} \text{ Å}^{-2}$ . The first 5 ns of each MD trajectory were designated to the final equilibration and were not included in the subsequent analysis. The total PMF profile of the dimer association was calculated by integrating the mean force  $\langle F(r) \rangle$ , where  $F(r)$  is the projection of the total force on the  $r$  vector.<sup>21</sup> Error estimation for each run was done by dividing the MD trace into 5 parts, which were

used for an independent generation of the profiles. For each dimer, the PMF calculations were completed twice, with the resulting profiles representing the average.

**Calculation of Partial Energy Contributions.** Protein, lipid, and water contributions into the dimerization free energy were assessed using the following technique: the original trajectory was converted to keep only a part of the system (protein or protein+lipids), and the forces acting on atoms were recalculated using the GROMACS *mdrun* utility. PMF profiles were obtained as described above. To get the components of interest, the curves can be added or subtracted. To estimate the contribution of a given subset of protein atoms (e.g., different parts of TM helices), the forces were extracted

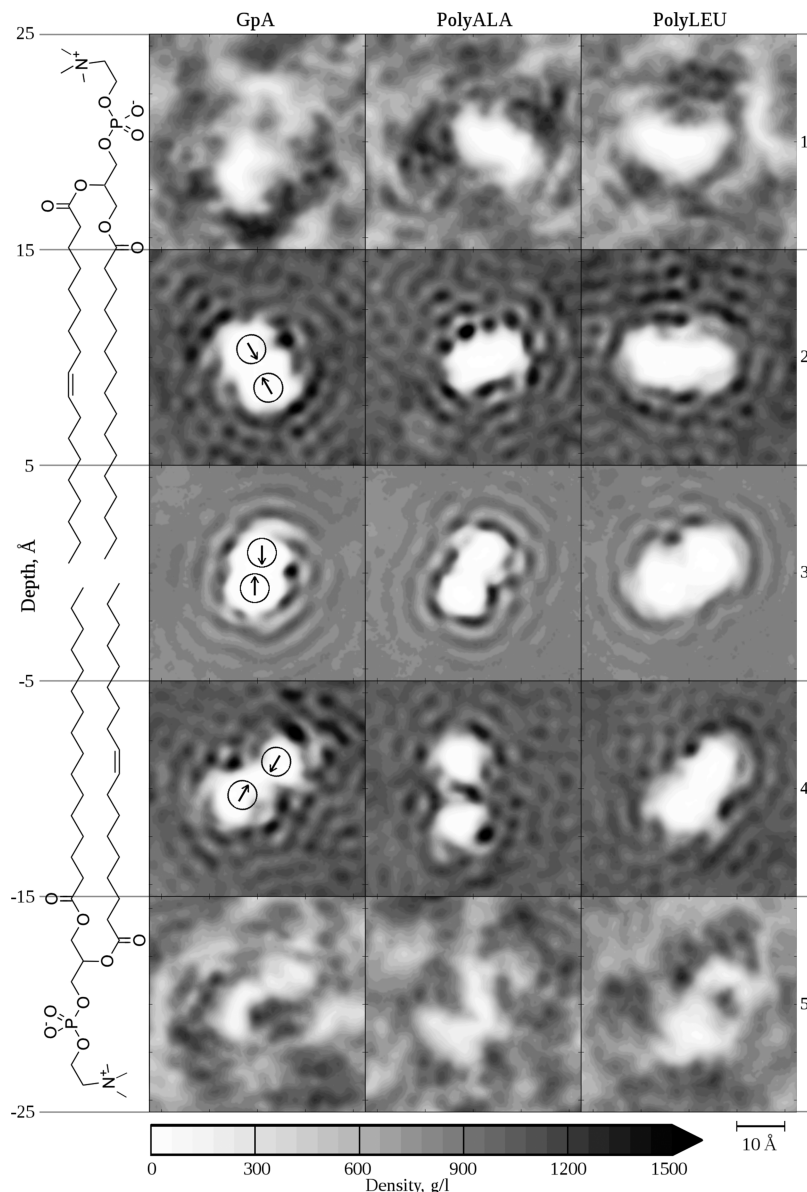


**Figure 3.** Average density distribution for the slices carved along the membrane normal of the POPC bilayer containing dimers of GpA (left), PolyALA (center), and PolyLEU (right) peptides at their equilibrium distance. Designations are the same as in Figure 2.

from the trajectory, averaged, and integrated. Note that for charged residues the procedure can result in overestimated values in cases where the solvent contributes strongly into the total interaction energy. The values corresponding to the distance of the lowest energy minimum were used in the preparation of all bar charts (Figure 1).

**Lipid Properties Analysis.** Lipid density was mapped in the  $(x, y)$  plane of the bilayer. 2D maps for 5 slices carved along the bilayer normal were treated separately. They correspond to lipid polar heads (top and bottom slices), the beginning of acyl chains (second and fourth slices), and acyl chains tails (middle slice). Density maps for the protein containing systems were calculated from 210 ns MD trajectories centered (by translation in the bilayer plane) with respect to a protein molecule and averaged over multiple MD frames (with the maximum number of 100000 frames, corresponding to 200 ns of MD run). First 10 ns of each trajectory were not taken into account. Periodic boundary conditions were taken into account. Lipid density was calculated as a mass density on a cubic grid with a step of  $0.5 \text{ \AA}$

and visualized using a Python script. For the maps shown in Figure 2, 3, S2, S3, and S4 a single MD trajectory was used in each case, for which calculated heterogeneity of lipid densities distribution (see below) in the middle slice is closest to the respective average values among three independent replicas. To test the effect of the averaging time-window on the heterogeneity of lipid density distributions (see below) additional grids corresponding to 10, 20, 50, and 100 ns of MD (5000, 10000, 25000, and 50000 frames, respectively) were also calculated for each trajectory.

#### Estimation of the Heterogeneity of the Lipid Density Distribution.

The heterogeneity of the lipid density distribution in each membrane slice was estimated according to the Shannon formula for the entropy of a distribution

$$H_{slice} = \sum_i^{Nbins} p_i \log_2 p_i \quad (1)$$

where  $p_i$  corresponds to the normalized probability of finding a density value in the  $i^{\text{th}}$  bin, and  $N_{\text{bins}}$  is the number of bins used to get a normalized lipid density distribution between 0 and 1500 g/L. Fifteen bins were selected as the optimal number of bins. The parameter  $H$  for the whole bilayer was calculated as the sum of these parameters for individual bilayer slices. These parameters were calculated for each MD trajectories independently and averaged over three MD replicas. A dependence of heterogeneity values on the time-widow for averaging is shown in Figure S5. Although absolute values of overall and the middle slice heterogeneities depend on time of averaging (Figure S5, upper panels), the general trends in how different peptides perturb packing of lipids stays rather stable. The heterogeneity of the pure bilayer equalizes faster with an increase of the averaging time as compared to peptide containing systems. This is why the heterogeneity of these systems relative to pure POPC displays a growth during MD (Figure S5, other panels). The final heterogeneity values were calculated from the grids averaged over 200 ns (200000 conformations) and relative to those parameters in the pure POPC, which are  $37.92 \pm 0.43$  and  $5.80 \pm 0.01$  for the whole bilayer and for the middle slice, respectively. The heterogeneity change upon dimerization was defined as the difference between these parameters calculated for three independent replicas of systems with interhelical distance of 8 and 22 Å, respectively, and averaged over nine possible deltas.

**Calculations of Lipid Conformational Entropy.** The conformational entropy of lipids was calculated using two independent techniques – the quasi-harmonic (QH) approach based on mass-weighted covariance matrices in Cartesian coordinates<sup>51</sup> and the mutual information approach, which employs MD-based distributions of lipid internal coordinates. For the latter calculation, a modified parallel version of the ENTROPICAL program<sup>52</sup> was used. Here, only part of the total conformational entropy corresponding to the dihedral angles contribution was considered. QH entropies were calculated using the *g\_covar* and *g\_anaeig* utilities from the GROMACS package and *Linux* scripts specially written for this purpose. Both approaches were applied separately to each lipid molecule. This was done using 100000 MD conformations of each lipid molecule in each simulated system. For the calculations of QH entropies, the rotational and translational degrees of freedom were removed using a least-squares fitting to average MD conformations of lipids. For each system, the average QH ( $S_{\text{conf}}^{\text{QH}}$ ) and dihedral ( $S_{\text{conf}}^{\text{dihedral}}$ ) conformational entropies were calculated per lipid molecule and also averaged over three independent replicas. All the reported conformational entropy values were evaluated relative to those in the “pure” POPC bilayer. The conformational entropy change upon dimerization was determined as the difference between these parameters calculated for three independent replicas of systems with interhelical distances of 8.0 and 22 Å, respectively, and averaged over nine possible deltas.

## ■ RESULTS

**Dimerization Free Energies.** The PMF profiles averaged over two independent simulations are shown in Figure 1A. The results are well converged and provide a direct estimate of the relative ability of the model helices to associate. As seen from the figure, the peptides display different dimerization strengths. For the strongest dimer of GpA, the PMF profile has a prominent minimum of  $-60 \pm 3$  kJ mol<sup>-1</sup>, while the dimerization free energies for PolyALA and PolyLEU are

similar and relatively weak ( $-14 \pm 3$  kJ mol<sup>-1</sup>). This is in line with available experimental and computational results reported elsewhere.<sup>18,21</sup> According to the PMF profile shapes, PolyALA tends to form a tightly packed dimer similar to GpA (the prominent minimum at small helix–helix separation), although significantly weaker. By contrast, the PolyLEU PMF profile drastically differs from the others, appearing as a broad “basin”. Thus, the free energy calculations allow classifying the modeled dimers as tightly packed and strong (GpA), tightly packed and weak (PolyALA), and “loose” (PolyLEU). In order to understand the detailed contribution of amino acid composition, lipids, and water to the free energy of helix–helix association, we extract individual energy terms corresponding to protein–protein, protein–lipid, and protein–water interactions. We assess these contributions independently for different fragments of the model peptides, starting from the central part of TM helices (residues 78–89 in GpA sequence), which resides within the acyl chain region of the bilayer (Figure 1B), to the whole-length peptides with a step of one residue added to N- and C-termini, respectively. The dependence of individual contributions on the fragments length displays complex and relatively unstable behavior (Figure 1C). Particularly, the inclusion of charged TM-flanking regions leads to a significant increase in the magnitude of individual components due to the strong impact of electrostatic interactions (some fragments with charged residues are not shown in the panel 1C for the clarity). Being large in absolute value, the contributions of the whole-length dimer interactions with water and lipids cancel each other out resulting in a relatively small magnitude of the total dimerization free energy. Surprisingly, the total free-energy gains for the central fragments (especially, residues 77–90) provide the same ranking of the dimers as those obtained for the whole-length peptides (see also Figure S1 for detailed PMF profiles of the central fragment). In other words, the characteristic interactions of the central TM fragments with each other and with the environment can potentially predefine the dimerization behavior of the whole-length peptide, while the contribution of regions residing in the highly heterogeneous water–lipid interface seems to be less specific and mostly demonstrates fluctuations of the free energy of association.

A detailed analysis of TM dimer interactions within the hydrophobic core of the bilayer gives a clear picture of the particular contribution of protein–protein and protein–lipid components into the dimerization free energy since the protein–water component is almost negligible here (Figure S1D). Thus, interactions within the dimers provide rather expected ranking according to favorable free-energy gains, namely, GpA > PolyALA > PolyLEU (Figure 1C), which can be explained by the efficiency of TM helices’ packing, mostly due to their surface geometry (see above). At the same time, the lipid component is significantly favorable for GpA and decreases its total dimerization free energy to a substantially lower value compared with other model peptides (Figure 1C). The contribution of protein–membrane interactions is smaller in the case of PolyLEU and even becomes unfavorable for PolyALA (Figures 1C, S1C). According to these results, the membrane modulates the dimerization strength of the model dimers, and its contribution is equally important to protein–protein interactions.

**Perturbation of the Lipid Packing by TM Peptides.** To better understand the particular nature of membrane impact on the dimerization of the peptides, we analyze in-plane

distributions of the lipid density for a number of bilayer slices carved along the normal (see [Methods](#) for details). First, we compare this property for monomers with the “pure” POPC bilayer used as a control ([Figure 2](#)). As seen from the figure, the presence of TM helices perturbs the lipid packing, which is reflected in a nonuniform distribution of the lipid density. Interestingly, the most prominent effect is observed for slices corresponding to the hydrophobic core of the bilayer ([Figure 2](#), middle panels). Here, the distribution is rather diffuse for the pure bilayer, thus ensuring an efficient averaging of the density during the observation period (200 ns), while some characteristic patterns can be observed for the monomers. Particularly, the presence of a TM helix results in the formation of concentric heterogeneities, where dark areas reflect a high average lipid density corresponding to immobilized lipid tails tightly bound to the peptide or constrained by the inclusion (i.e., TM peptide). The restriction of acyl chain atoms in their spatial location during MD leads consequently to a depletion of neighboring regions and the formation of “ring-like” structures upon averaging. The most prominent density peaks – some analogous to the first solvation shell in liquids – are located in direct proximity to the peptides, with the effect gradually decaying at larger distances.

The monomers perturb the hydrophobic core in a sequence-specific manner. Thus, in the case of GpA this perturbation has an asymmetric character ([Figure 2](#), slice 3) – high-density regions concentrate around hydrophobic residues (M81, A82, V84, I85), while the vicinity of polar residues (GpA dimerization interface: G83, G86, T87) is depleted by acyl chain atoms (see also [Figure S2B](#)). These heterogeneities create a first “solvation shell” with the characteristic radius of about 8 Å. In the case of PolyALA and PolyLEU homopolymers the density distribution has a symmetric structure with characteristic sizes of the first high-density region of 7 and 10 Å, respectively ([Figure 2](#), slice 3). For PolyALA, the perturbation pattern contains five prominent density maxima. Although similar features still remain for the upper and lower slices ([Figure 2](#), slices 2, 4) corresponding to carbonyl groups and the beginning of acyl chain regions, the perturbations are less dramatic here compared with the pure bilayer. Moreover, the difference between the membrane with and without inclusions is almost negligible for the top and bottom slices ([Figure 2](#), slices 1, 5) corresponding to the water–lipid interface. The latter phenomenon can be explained by the fact that the region of lipid polar heads already has a highly heterogeneous nature in the “pure” POPC bilayer, where molecular-size POPC clusters may exist.<sup>45</sup> This is why peptide inclusions do not increase the heterogeneity of the water–lipid interface but rather redistribute high- and low-density regions. In contrast, acyl chains are much more flexible, giving an almost uniform density distribution on the averaging interval and lacking strong interactions compared to the electrostatic ones in the interface. However, the apparent “gas-like” hydrophobic core in the bilayer region is most sensitive to the presence of the inclusions, which assures discrimination between different surface geometries and properties of TM helices encoded in their amino acid sequences.

How does the lipid perturbation change upon the dimerization of TM helices? As seen from [Figure 3](#), the most prominent differences between the simulated dimers correspond again to the middle membrane slice. When two peptides come closer, the aforementioned lipid density patterns become overlapped at distances of about 18–20 Å ([Figures S3, S4](#)).

There is no direct protein–protein contact at that stage, but the lipid perturbations start to evolve. New density maxima appear as monomers approach each other, and the “interfacial” maximum vanishes at a distance of 10–12 Å. Interestingly, the density distribution becomes more symmetric upon dimerization for GpA, while the symmetry is somehow broken for PolyLEU and, especially for PolyALA ([Figure 3](#), middle slice). In the case of GpA the effect can be explained by the reorganization of the TM helices’ surface exposed to the lipid environment: the polar residues (e.g., G83, T87) colocalized in the monomer ([Figure 3](#), middle slice) with low-density membrane regions are getting buried on the dimer interface as the helices come close together, which increases the fraction of exposed hydrophobic residues and gradually remodels the density distribution (see also [Figures S3, S4](#)). The latter results in the formation of a high lipid-density shell encompassing the dimer. Thus, protein atoms in the dimer fill the cavities present in close vicinity of the GpA monomer. On the contrary, the initial symmetry of perturbation patterns for the homopolymer helices decreases due to a loss of regularity of the dimer surfaces.

**Changes in Heterogeneity of Lipid Packing upon Dimerization: Shannon-Type Description.** In order to quantify the lipid perturbation induced by TM helices, we calculate Shannon entropies of the density distributions for all simulated systems. The resulting  $H$  values calculated according [eq 1](#) (see [Methods](#) for details) are attributed to heterogeneity of lipid packing density (hereinafter referred as “heterogeneity”). As one can see from [Figure S5](#) (upper panels) the overall and middle slice heterogeneity of the pure bilayer equalizes faster with increasing of the averaging time than in the case of peptide containing systems. This results in a growth of the heterogeneity obtained for monomer and dimer systems relative to pure POPC ([Figure S5](#), other panels), while the observing trends are relatively stable. For final analysis, we use heterogeneity values obtained from 200 ns averaged density grids. As it was mentioned before heterogeneities are higher for the membranes containing monomers and dimers compared with the “pure” POPC bilayer ([Figure S8](#), upper panels).

The total relative heterogeneities for all systems nicely resemble the trend observed for those calculated only for the middle bilayer slice. Thus, the perturbation of the hydrophobic core of the bilayer induced by TM helices seems to almost predefine the character of the total effect. The heterogeneity level gradually increases for the monomers as follows: PolyALA < GpA < PolyLEU; however, the effect becomes more similar between the dimers ([Figure S8](#), upper panels). At the same time, for the dimers the total heterogeneity and that for the middle slice decrease upon dimerization ([Figure 4A](#)). The deltas are calculated between the dimeric systems with closely packed and far separated helices (see [Methods](#)) and provide rather stable ranking of the dimers on averaging time-windows above 25 ns (see [Figure S6](#)). The most prominent drop in the heterogeneity upon dimerization is observed for PolyLEU and the least one for PolyALA, while GpA displays an intermediate behavior as compared to both extremes ([Figure 4A](#)). In other words, PolyLEU has a strong ability to make the lipid density distribution more uniform upon association, while these tendencies are weaker for GpA and, especially, for PolyALA. Interestingly, we also observe a rather different behavior of PolyALA compared with PolyLEU and GpA when it comes to the protein–lipid component of the dimerization free energies for the central TM fragments ([Figures 1C and S1C](#)). However,

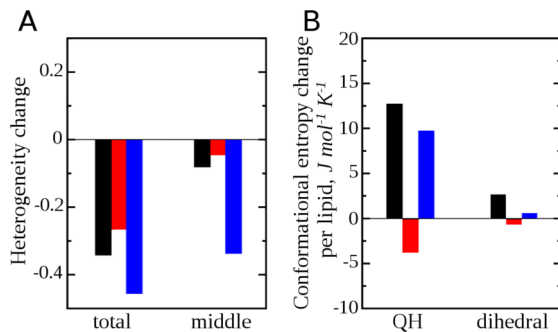


**Figure 4.** Changes in heterogeneity of lipid packing upon dimerization of GpA (black), PolyALA (red), and PolyLEU (blue) peptides in the POPC bilayer for the whole peptide (“total”) and its central part (“middle”) (A). Lipid conformational entropy changes upon dimerization calculated using the quasi-harmonic approach for Cartesian coordinates (“QH”) and using dihedral angle distributions (“dihedral”) (B).

the thermodynamic effect seems to be clearer than that estimated just from perturbation of the lipid packing.

**Entropic Effect of Dimerization.** How is the entropy of lipids connected to the heterogeneity of their packing and the particular contribution of protein–lipid interactions to the dimerization free energy? To answer this question, we calculate the average conformational entropy per lipid molecule ( $S_{\text{conf}}$ ) in all simulated systems using two independent techniques – the quasi-harmonic approach for Cartesian coordinates of lipids<sup>51</sup> (QH) and the histogram approach using the MD distributions of their dihedral angles.<sup>52</sup> These two methods give well-correlated sets of conformational entropy values relative to pure POPC (Figure S7, Pearson correlation coefficient  $R^2$  is 0.8), while the magnitude is a few times higher for QH. Such a behavior of two entropy estimation approaches used here is in-line with the known fact that QH gives an upper bound of conformational entropy, while the entropy approximated just based on dihedral angles’ distributions usually represents an underestimate of the real value.<sup>18,53</sup>

First, we observed that both  $S_{\text{conf}}\text{-QH}$  and  $S_{\text{conf}}\text{-dihedral}$  are decreased by monomers as compared to the “pure” bilayer (Figure S8, lower panels), and this effect has a reverse correspondence to the observed heterogeneity increase upon monomer inclusions (Figure S8, upper panels). The change in both conformational entropies is also negative for all dimers as compared to the pure bilayer. However, we observe key differences in the entropic effect upon dimerization (the deltas calculated between the dimeric systems with closely packed and far separated helices, see Methods). As seen from Figure 4B, the dimerization of GpA has a favorable entropic effect, which is estimated according to changes in both  $S_{\text{conf}}\text{-QH}$  and  $S_{\text{conf}}\text{-dihedral}$  values. The opposite is true for PolyALA. For PolyLEU the decrease of the lipid conformational entropy is similar to GpA yet less prominent. Although the conformational entropy changes for lipids upon dimer formation do not absolutely follow the respective heterogeneity changes, they are in a good agreement with estimates of the impact of protein–lipid interaction on the dimerization free energy (see above). For instance, a decrease of the heterogeneity of the lipid density distribution upon GpA dimer formation is associated with a substantial increase of the lipid conformational entropy and corresponds to the prominently favorable effect of protein–lipid interactions on the dimerization free energy for the central TM fragments (Figure 1C). In other words, in this particular

case the dimerization of GpA helices reduces constraints for acyl chains, which leads to an increase of the lipid conformational entropy, while the two effects are still not quantitative equivalents of each other.

## DISCUSSION

The most intriguing result of this study is that the membrane can potentially drive the self-association (dimerization) of TM helices of different proteins, while protein–protein interactions can play a secondary role (at least for the TM helices studied here). Such a conclusion is rather different from the common view that only sequence motifs in TM peptides play a dominant role in the dimerization and in ensuring tight helix packing. Our data extend such a concept and outline that the amino acid sequence is important because it provides at least two prerequisites for peptide association. First, it is important for the proper folding and insertion of the peptide – the well-known factors here are sufficiently high propensities of residues to form an  $\alpha$ -helix in the membrane environment, presence of “anchoring” polar and charged residues on the peptide termini to adopt a TM orientation, the preferential distribution of some types of residues (e.g., aromatic) near the water–lipid interface, and so on. Second, the peptide sequence determines a suitable dynamic landscape on the peptide surface, which predefines both interactions with a peptide counterpart and the environment. If the latter facilitates an entropically favorable arrangement of lipid acyl chains in the dimer vicinity, the dimerization potency of a peptide can be amplified like in a case of GpA. In contrast, short protein side chains (like in case of PolyALA) hamper its interactions with surrounding lipids and hence diminish the dimerization ability of the helix. Interestingly, different characteristic patterns of perturbation in lipid packing near the helix surface are already observed for TM helical monomers.

The fact that the dimerization strength of TM peptides with a given sequence can be strongly modulated by the lipid environment has already been shown experimentally and computationally,<sup>18,37,38</sup> but molecular details of such effects still remain poorly understood. In the present study, we indeed observe that the presence of the G<sub>4</sub> motif in the GpA central TM fragment (e.g., residues 78–89) allows for the most favorable contribution of protein–protein interactions to the dimerization free energy as compared to other model peptides (Figures 1C and S1). However, this effect is not dramatically different from the strength of protein–protein interactions in PolyALA and PolyLEU dimers. Hence, it does not explain solely the few fold difference between the total dimerization energy of GpA and the homopolymers (Figures 1C and S1). Here, the contribution of protein–lipid interactions is favorable and equally strong for the protein component of GpA and significantly increases its association strength; it dominates in the dimerization of the PolyLEU fragment; it is, however, unfavorable for PolyALA, weakening the association of the latter dimer. The hydrophobic core of the bilayer displays a prominent sensitivity to the particular amino-acid composition of TM fragments and is able to modulate their dimerization in a sequence-specific manner. This effect is particularly interesting, given the relatively homogeneous and apparent “gas-like” organization of this lipid matrix.

In contrast to peripheral regions of the bilayer, none of the strong interactions such as hydrogen bonds or electrostatic contacts are present in its core, and the “recognition” of different TM peptides can be served only by the collective

dynamic response of lipid tails to the presence of the inclusion. In the present study, we estimate the membrane response to a perturbation of the lipid packing by TM helices, which is reflected in the nonuniform character of in-plane distributions of the lipid density. Similar effects have been observed for the integrins.<sup>54</sup> The fact that the inclusions induced perturbations in the bilayer with the shape of a damped oscillation, which mediate the interaction between TM objects, has also been reported for coarse-grained lattice models.<sup>55</sup> According to our fine-resolution data, the most dramatic effect of monomer inclusion compared to the pure POPC bilayer is observed for the middle membrane slice, which corresponds to the hydrophobic core (**Figure 2**) and the same is true for the helices association (**Figures 3, S2, and S3**). Of course, the interactions within the water–lipid interface also contribute to the dimerization, but we specifically focus on the effects occurring in the membrane interior – in order to get a clear model of the sequence-specific modulation of the dimerization provided by lipids. Thus, the presence of a monomeric TM helix induces large-scale perturbations of the hydrophobic core that leads to the formation of characteristic patterns in 2D lipid density distribution – asymmetric in the case of GpA and symmetric for homopolymers (**Figure 2**).

Increase in the bilayer's heterogeneity according to the Shannon entropy of the lipid density distribution by the monomers corresponds also to a decrease in both measures of the lipid conformational entropies –  $S_{\text{conf}}^{\text{QH}}$  and  $S_{\text{conf}}^{\text{dihedral}}$  relative to the pure POPC, being most prominent for PolyLEU (**Figure S8**). Although the calculated conformational entropy of lipids does not describe the complete entropic effects of the inclusions due to the missing (at least partial) rotational and translational components, the fact that it is connected to the effects observed from the analysis of the lipid density, especially for the hydrophobic core of the bilayer (see e.g., middle slice for PolyLEU monomer, **Figure 2**), allows for getting rather consistent observations. The confined configurational space of lipid acyl chains results in decreasing lipid conformational entropy compared with the unperturbed state of the membrane (**Figure S8**). We should note that the entropy calculations used here do not give a precise estimate of the entropic effect of the insertion and dimerization of TM helices but rather describe a qualitative yet physically relevant picture and provide a link between the perturbation of the lipid packing and membrane thermodynamics. The value of absolute  $S_{\text{conf}}^{\text{QH}}$  estimated per lipid molecule in the pure POPC ( $2.926 \pm 0.007 \text{ kJ mol}^{-1} \text{ K}^{-1}$ ) corresponds well to the results obtained with the same approach for other phospholipids,<sup>56</sup> and, as shown in the mentioned study, the acyl chains contribute up to 70% to the conformational entropy.

Here, we also use the mutual information approach to estimate solely the contribution of dihedral angles to the conformational entropy ( $S_{\text{conf-dihedral}}$ ), which mostly captures the effects associated with acyl chains. Both calculations give qualitatively similar results, which together with the lipid density mapping provide a detailed understanding of the membrane's contribution to the dimerization of TM helices. Thus, upon association of PolyALA helices with the regular and ridged surface, the perturbation of the hydrophobic core increases (**Figures S3, S4**), which results in a highly contrasted density map obtained for the dimer (**Figure 3**) and is associated with the strongest lipid conformational entropy loss (**Figure 4**). This explains the unfavorable contribution of protein–lipid interactions into the dimerization free energy of PolyALA

(**Figures 1** and **S1**). The TM helix of another homopolymer – PolyLEU – in the monomeric state disturbs the packing of acyl chains even stronger due to the presence of long and flexible side chains. However, upon dimerization, the substantial reduction of the dimer's exposed surface leads to a relative decrease in the bilayer's heterogeneity, a smaller entropic penalty compared with PolyALA and a reduction in the dimerization free energy by the membrane component. Finally, the GpA TM helix has a surface optimized during the evolution and representing an appropriate combination of hydrophobic and small-side chain polar (Gly, Thr) residues, which moderately perturbs the bilayer interior in the monomeric state and provides a gain in lipid conformational entropy upon dimerization. Also, it facilitates the formation of the tightly packed dimer that makes an equally favorable contribution of protein–protein and protein–lipids interactions to the association free energy possible.

Why are large-scale perturbations of the lipid's structural organization and dynamic behavior inside the bilayer mostly responsible for the dimerization? As we show here, the lipid's polar heads are much less sensitive to membrane perturbations induced by the insertion of TM helices (**Figure 2**). Although the membrane surface exhibits a mosaic-like character caused by a lateral clustering of lipids,<sup>45</sup> such heterogeneities are highly dynamic (typical lifetime is about 1 ns). In contrast, lipid chains can be easily immobilized on the peptide surface and reside there for a relatively long time (up to 200 ns). As mentioned before, a possible explanation for these differences is the occurrence of strong intermolecular long-range electrostatic interactions observed in the bilayer's peripheral regions between protein residues, lipids, and water molecules, which rival each other. Such competitive long-range interactions are almost missing in the nonpolar region of the membrane. Therefore, the events considered to be the most important for dimerization occur in the hydrophobic core, while the polar head region serves as a peculiar buffer, protecting the membrane's surface and the surrounding water from the structural rearrangements occurring upon helix–helix association. The latter conclusions also corroborate our previous simulations of water dynamics near and inside lipid bilayers.<sup>57</sup>

An important inference from this work is related to the design of potential TM peptides, which are destined to modulate helix–helix association. Such peptides are called “interceptors”.<sup>58–60</sup> The problem is considered important because in the case of signal cell receptors (e.g., tyrosine kinases) such a regulation represents a novel innovative strategy to fight many serious diseases (see refs 59, 61, and 62 for review). Taking into account the results obtained, we assume that the development of the interceptors may be focused on the perturbation of the lipid packing near the peptide surface, e.g., via point mutations. In contrast to the previous strategies, the mutations should not necessarily lie on the helix–helix interface.<sup>63</sup> Moreover, they can be even located far away from it – the main idea is to change peptide-lipid interactions, thus promoting membrane-driven association in a predicted way.

In this study, we purposely do not explore the effects of lipid composition on TM helix association so as to simplify the system by eliminating one of the factors, whose role is difficult to account for in a proper way. At the same time, it is well-known that the chemical nature of lipids seriously affects the structure and dynamics of the respective bilayers, which can be drastically changed even due to minor changes in lipid composition.<sup>45,46</sup> Since we show here that the lipid matrix

governs TM helix dimerization, any phenomena resulting in the modification of lipid bilayer properties should be carefully taken into account. Obviously, this will complicate the current view and requires a special investigation in future, although the principal conclusions will hopefully remain quite similar.

Based on the presented data, we assume that two individual TM helices “feel” each other due to a perturbation of the lipid organization in the membrane. As we discuss above, the insertion of TM helices creates heterogeneities in the lateral lipid density distribution up to distances of about 20 Å from the helix’ axis, and thereafter the spatial scale of the lipid perturbations created by the helix pair is about 40 Å. At such separations, helices do not interact directly – the corresponding free energy profiles reach zero above 20–22 Å (Figures 1, S1). Therefore, the question still remains: How exactly do the helices recognize each other in the “lipid sea”? We realize that the presented picture of membrane-driven assembling of TM helices still does not bring to light any simple and comprehensible macroscopic factor (like force, etc.), which can unambiguously explain known dimerization events and predict new ones. This is beyond the scope of the present work. However, the results extend our understanding of the crucial role of the lipid matrix in the association of TM helices in membranes, as well as equalize the contributions of protein–protein and protein–membrane interactions into this process.

## CONCLUSION

The dimerization of membrane proteins is a complex process, which is highly important for the functioning of living cells. Although the most specific interactions occur between proteins, the lipid membrane also takes an active part in the association of transmembrane segments. Here, we show that even the simplest TM helices can induce a perturbation in the lipid bilayer in a sequence-specific manner. In response to the perturbation, the lipid matrix can promote the association of TM helices mainly due to the entropic nature of the effect. Even in the case of such a strong dimer as glycophorin A, whose association is thought to be almost exclusively predefined by an efficient packing of TM helices, the lipids play a substantial role in its dimerization.

## ASSOCIATED CONTENT

### Supporting Information

The Supporting Information is available free of charge on the ACS Publications website at DOI: [10.1021/acs.jctc.5b00206](https://doi.org/10.1021/acs.jctc.5b00206).

Figures S1–S8 (PDF)

## AUTHOR INFORMATION

### Corresponding Author

\*E-mail: [r-efremov@yandex.ru](mailto:r-efremov@yandex.ru).

### Author Contributions

The manuscript was written through contributions of all authors.

### Funding

This work was supported by the Russian Scientific Foundation (grant 14-14-00871 awarded to R.G.E.).

### Notes

The authors declare no competing financial interest.

## ACKNOWLEDGMENTS

Access to the computational facilities of the Joint Supercomputer Center of RAS (Moscow) is greatly appreciated. The authors thank Ms. Anastasia Efremova for editing the manuscript and Mr. Nikolay Krylov for assistance with data processing.

## ABBREVIATIONS

GpA, glycophorin A; MD, molecular dynamics; PMF, potential of mean force; PolyALA, polyalanine; PolyLEU, polyleucine; POPC, palmitoyloleylphosphatidylcholine; QH, quasi-harmonic approach; TM, transmembrane

## REFERENCES

- Bergsagel, P. L.; Chesi, M. V. Molecular Classification and Risk Stratification of Myeloma. *Hematol. Oncol.* **2013**, *31*, 38–41.
- Al Hussain, T. O.; Akhtar, M. Molecular Basis of Urinary Bladder Cancer. *Adv. Anat. Pathol.* **2013**, *20*, 53–60.
- Nikonov, A. V.; Kreibich, G. Organization of Translocon Complexes in ER Membranes. *Biochem. Soc. Trans.* **2003**, *31*, 1253–1256.
- Fleming, K. G. Energetics of Membrane Protein Folding. *Annu. Rev. Biophys.* **2014**, *43*, 233–255.
- Nyathi, Y.; Wilkinson, B. M.; Pool, M. R. Co-Translational Targeting and Translocation of Proteins to the Endoplasmic Reticulum. *Biochim. Biophys. Acta, Mol. Cell Res.* **2013**, *1833*, 2392–2402.
- Schlebach, J. P.; Sanders, C. R. The Safety Dance: Biophysics of Membrane Protein Folding and Misfolding in a Cellular Context. *Q. Rev. Biophys.* **2015**, *48*, 1–34.
- Jura, N.; Endres, N. F.; Engel, K.; Deindl, S.; Das, R.; Lamers, M. H.; Wemmer, D. E.; Zhang, X.; Kuriyan, J. Mechanism for Activation of the EGF Receptor Catalytic Domain by the Juxtamembrane Segment. *Cell* **2009**, *137*, 1293–1307.
- Bae, J. H.; Schlessinger, J. Asymmetric Tyrosine Kinase Arrangements in Activation or Autophosphorylation of Receptor Tyrosine Kinases. *Mol. Cells* **2010**, *29*, 443–448.
- MacKenzie, K. R.; Prestegard, J. H.; Engelman, D. M. A Transmembrane Helix Dimer: Structure and Implications. *Science* **1997**, *276*, 131–133.
- Bocharov, E. V.; Lesovoy, D. M.; Goncharuk, S. A.; Goncharuk, M. V.; Hristova, K.; Arseniev, A. S. Structure of FGFR3 Transmembrane Domain Dimer: Implications for Signaling and Human Pathologies. *Structure* **2013**, *21*, 2087–2093.
- Mineev, K. S.; Lesovoy, D. M.; Usmanova, D. R.; Goncharuk, S. A.; Shulepko, M. A.; Lyukmanova, E. N.; Kirpichnikov, M. P.; Bocharov, E. V.; Arseniev, A. S. NMR-Based Approach to Measure the Free Energy of Transmembrane Helix–helix Interactions. *Biochim. Biophys. Acta, Biomembr.* **2014**, *1838*, 164–172.
- Bocharov, E. V.; Mayzel, M. L.; Volynsky, P. E.; Mineev, K. S.; Tkach, E. N.; Ermolyuk, Y. S.; Schulga, A. A.; Efremov, R. G.; Arseniev, A. S. Left-Handed Dimer of EphA2 Transmembrane Domain: Helix Packing Diversity among Receptor Tyrosine Kinases. *Biophys. J.* **2010**, *98*, 881–889.
- Bocharov, E. V.; Mineev, K. S.; Goncharuk, M. V.; Arseniev, A. S. Structural and Thermodynamic Insight into the Process of “weak” Dimerization of the ErbB4 Transmembrane Domain by Solution NMR. *Biochim. Biophys. Acta, Biomembr.* **2012**, *1818*, 2158–2170.
- Endres, N. F.; Das, R.; Smith, A. W.; Arkhipov, A.; Kovacs, E.; Huang, Y.; Pelton, J. G.; Shan, Y.; Shaw, D. E.; Wemmer, D. E.; Groves, J. T.; Kuriyan, J. Conformational Coupling across the Plasma Membrane in Activation of the EGF Receptor. *Cell* **2013**, *152*, 543–556.
- Engelman, D. M.; Adair, B. D.; Brünger, A.; Flanagan, J. M.; Hunt, J. F.; Lemmon, M. A.; Treutlein, H.; Zhang, J. Dimerization of Glycophorin A Transmembrane Helices: Mutagenesis and Modeling. *Soc. Gen. Physiol. Ser.* **1993**, *48*, 11–21.

- (16) Fleming, K. G.; Engelman, D. M. Specificity in Transmembrane Helix-Helix Interactions Can Define a Hierarchy of Stability for Sequence Variants. *Proc. Natl. Acad. Sci. U. S. A.* **2001**, *98*, 14340–14344.
- (17) Vereshaga, Y. A.; Volynsky, P. E.; Nolde, D. E.; Arseniev, A. S.; Efremov, R. G. Helix Interactions in Membranes: Lessons from Unrestrained Monte Carlo Simulations. *J. Chem. Theory Comput.* **2005**, *1*, 1252–1264.
- (18) Polyansky, A. A.; Volynsky, P. E.; Efremov, R. G. Multistate Organization of Transmembrane Helical Protein Dimers Governed by the Host Membrane. *J. Am. Chem. Soc.* **2012**, *134*, 14390–14400.
- (19) Volynsky, P. E.; Polyansky, A. A.; Fakhrutdinova, G. N.; Bocharov, E. V.; Efremov, R. G. Role of Dimerization Efficiency of Transmembrane Domains in Activation of Fibroblast Growth Factor Receptor 3. *J. Am. Chem. Soc.* **2013**, *135*, 8105–8108.
- (20) Polyansky, A. A.; Chugunov, A. O.; Volynsky, P. E.; Krylov, N. A.; Nolde, D. E.; Efremov, R. G. PREDDIMER: A Web Server for Prediction of Transmembrane Helical Dimers. *Bioinformatics* **2014**, *30*, 889–890.
- (21) Hénin, J.; Pohorille, A.; Chipot, C. Insights into the Recognition and Association of Transmembrane Alpha-Helices. The Free Energy of Alpha-Helix Dimerization in Glycophorin A. *J. Am. Chem. Soc.* **2005**, *127*, 8478–8484.
- (22) MacKenzie, K. R.; Engelman, D. M. Structure-Based Prediction of the Stability of Transmembrane Helix-Helix Interactions: The Sequence Dependence of Glycophorin A Dimerization. *Proc. Natl. Acad. Sci. U. S. A.* **1998**, *95*, 3583–3590.
- (23) Park, S.; Im, W. Two Dimensional Window Exchange Umbrella Sampling for Transmembrane Helix Assembly. *J. Chem. Theory Comput.* **2013**, *9*, 13–17.
- (24) Melnyk, R. A.; Kim, S.; Curran, A. R.; Engelman, D. M.; Bowie, J. U.; Deber, C. M. The Affinity of GXXXG Motifs in Transmembrane Helix-Helix Interactions Is Modulated by Long-Range Communication. *J. Biol. Chem.* **2004**, *279*, 16591–16597.
- (25) Doura, A. K.; Kobus, F. J.; Dubrovsky, L.; Hibbard, E.; Fleming, K. G. Sequence Context Modulates the Stability of a GXXXG-Mediated Transmembrane Helix–Helix Dimer. *J. Mol. Biol.* **2004**, *341*, 991–998.
- (26) Cymer, F.; Veerappan, A.; Schneider, D. Transmembrane Helix-Helix Interactions Are Modulated by the Sequence Context and by Lipid Bilayer Properties. *Biochim. Biophys. Acta, Biomembr.* **2012**, *1818*, 963–973.
- (27) Mineev, K. S.; Khabibullina, N. F.; Lyukmanova, E. N.; Dolgikh, D. A.; Kirpichnikov, M. P.; Arseniev, A. S. Spatial Structure and Dimer–monomer Equilibrium of the ErbB3 Transmembrane Domain in DPC Micelles. *Biochim. Biophys. Acta, Biomembr.* **2011**, *1808*, 2081–2088.
- (28) Duneau, J.-P.; Vegh, A. P.; Sturgis, J. N. A Dimerization Hierarchy in the Transmembrane Domains of the HER Receptor Family. *Biochemistry* **2007**, *46*, 2010–2019.
- (29) Russ, W. P.; Engelman, D. M. TOXCAT: A Measure of Transmembrane Helix Association in a Biological Membrane. *Proc. Natl. Acad. Sci. U. S. A.* **1999**, *96*, 863–868.
- (30) Chipot, C. Free Energy Calculations Applied to Membrane Proteins. *Methods Mol. Biol.* **2008**, *443*, 121–144.
- (31) Pohorille, A.; Jarzynski, C.; Chipot, C. Good Practices in Free-Energy Calculations. *J. Phys. Chem. B* **2010**, *114*, 10235–10253.
- (32) Polyansky, A. A.; Volynsky, P. E.; Efremov, R. G. Structural, Dynamic, and Functional Aspects of Helix Association in Membranes: A Computational View. *Adv. Protein Chem. Struct. Biol.* **2011**, *83*, 129–161.
- (33) Smith, S. O.; Eilers, M.; Song, D.; Crocker, E.; Ying, W.; Groesbeek, M.; Metz, G.; Ziliox, M.; Aimoto, S. Implications of Threonine Hydrogen Bonding in the Glycophorin A Transmembrane Helix Dimer. *Biophys. J.* **2002**, *82*, 2476–2486.
- (34) Lee, J.; Im, W. Role of Hydrogen Bonding and Helix-Lipid Interactions in Transmembrane Helix Association. *J. Am. Chem. Soc.* **2008**, *130*, 6456–6462.
- (35) Anbazhagan, V.; Schneider, D. The Membrane Environment Modulates Self-Association of the Human GpA TM domain—Implications for Membrane Protein Folding and Transmembrane Signaling. *Biochim. Biophys. Acta, Biomembr.* **2010**, *1798*, 1899–1907.
- (36) Hong, H.; Blois, T. M.; Cao, Z.; Bowie, J. U. Method to Measure Strong Protein-Protein Interactions in Lipid Bilayers Using a Steric Trap. *Proc. Natl. Acad. Sci. U. S. A.* **2010**, *107*, 19802–19807.
- (37) Hong, H.; Bowie, J. U. Dramatic Destabilization of Transmembrane Helix Interactions by Features of Natural Membrane Environments. *J. Am. Chem. Soc.* **2011**, *133*, 11389–11398.
- (38) Janosi, L.; Prakash, A.; Doxastakis, M. Lipid-Modulated Sequence-Specific Association of Glycophorin A in Membranes. *Biophys. J.* **2010**, *99*, 284–292.
- (39) Caputo, G. A. Analyzing the Effects of Hydrophobic Mismatch on Transmembrane A-Helices Using Tryptophan Fluorescence Spectroscopy. *Methods Mol. Biol.* **2013**, *1063*, 95–116.
- (40) Prakash, A.; Janosi, L.; Doxastakis, M. GXXXG Motifs, Phenylalanine, and Cholesterol Guide the Self-Association of Transmembrane Domains of ErbB2 Receptors. *Biophys. J.* **2011**, *101*, 1949–1958.
- (41) Lensink, M. F.; Govaerts, C.; Ruyschaert, J.-M. Identification of Specific Lipid-Binding Sites in Integral Membrane Proteins. *J. Biol. Chem.* **2010**, *285*, 10519–10526.
- (42) Poveda, J. A.; Giudici, A. M.; Renart, M. L.; Molina, M. L.; Montoya, E.; Fernández-Carvajal, A.; Fernández-Ballester, G.; Encinar, J. A.; González-Ros, J. M. Lipid Modulation of Ion Channels through Specific Binding Sites. *Biochim. Biophys. Acta, Biomembr.* **2014**, *1838*, 1560–1567.
- (43) Sharma, S.; Lensink, M. F.; Juffer, A. H. The Structure of the CD3 $\zeta\zeta$  Transmembrane Dimer in Lipid Bilayers. *Biochim. Biophys. Acta, Biomembr.* **2014**, *1838*, 739–746.
- (44) Prasanna, X.; Chattopadhyay, A.; Sengupta, D. Cholesterol Modulates the Dimer Interface of the  $\beta$ 2-Adrenergic Receptor via Cholesterol Occupancy Sites. *Biophys. J.* **2014**, *106*, 1290–1300.
- (45) Pyrkova, D. V.; Tarasova, N. K.; Krylov, N. A.; Nolde, D. E.; Pentkovsky, V. M.; Efremov, R. G. Dynamic Clustering of Lipids in Hydrated Two-Component Membranes: Results of Computer Modeling and Putative Biological Impact. *J. Biomol. Struct. Dyn.* **2013**, *31*, 87–95.
- (46) Parton, D. L.; Tek, A.; Baaden, M.; Sansom, M. S. P. Formation of Raft-like Assemblies within Clusters of Influenza Hemagglutinin Observed by MD Simulations. *PLoS Comput. Biol.* **2013**, *9*, e1003034.
- (47) Mineev, K. S.; Bocharov, E. V.; Volynsky, P. E.; Goncharuk, M. V.; Tkach, E. N.; Ermolyuk, Y. S.; Schulga, A. A.; Chupin, V. V.; Maslennikov, I. V.; Efremov, R. G.; Arseniev, A. S. Dimeric Structure of the Transmembrane Domain of Glycophorin a in Lipidic and Detergent Environments. *Acta Naturae* **2011**, *3*, 90–98.
- (48) Van Der Spoel, D.; Lindahl, E.; Hess, B.; Groenhof, G.; Mark, A. E.; Berendsen, H. J. C. GROMACS: Fast, Flexible, and Free. *J. Comput. Chem.* **2005**, *26*, 1701–1718.
- (49) Bussi, G.; Donadio, D.; Parrinello, M. Canonical Sampling through Velocity Rescaling. *J. Chem. Phys.* **2007**, *126*, 014101.
- (50) Berendsen, H. J. C.; Postma, J. P. M.; van Gunsteren, W. F.; DiNola, A.; Haak, J. R. Molecular Dynamics with Coupling to an External Bath. *J. Chem. Phys.* **1984**, *81*, 3684.
- (51) Andricioaei, I.; Karplus, M. On the Calculation of Entropy from Covariance Matrices of the Atomic Fluctuations. *J. Chem. Phys.* **2001**, *115*, 6289–6292.
- (52) Numata, J.; Knapp, E.-W. Balanced and Bias-Corrected Computation of Conformational Entropy Differences for Molecular Trajectories. *J. Chem. Theory Comput.* **2012**, *8*, 1235–1245.
- (53) Baron, R.; McCammon, J. A. (Thermo)dynamic Role of Receptor Flexibility, Entropy, and Motional Correlation in Protein–Ligand Binding. *ChemPhysChem* **2008**, *9*, 983–988.
- (54) Mehrbod, M.; Mofrad, M. R. K. Localized Lipid Packing of Transmembrane Domains Impedes Integrin Clustering. *PLoS Comput. Biol.* **2013**, *9*, e1002948.
- (55) Kik, R. A.; Leermakers, F. A. M.; Kleijn, J. M. Molecular Modeling of Proteinlike Inclusions in Lipid Bilayers: Lipid-Mediated Interactions. *Phys. Rev. E Stat. Nonlin. Soft Matter Phys.* **2010**, *81*, 021915.

- (56) Baron, R.; de Vries, A. H.; Hünenberger, P. H.; van Gunsteren, W. F. Configurational Entropies of Lipids in Pure and Mixed Bilayers from Atomic-Level and Coarse-Grained Molecular Dynamics Simulations. *J. Phys. Chem. B* **2006**, *110*, 15602–15614.
- (57) Krylov, N. A.; Pentkovsky, V. M.; Efremov, R. G. Nontrivial Behavior of Water in the Vicinity and inside Lipid Bilayers as Probed by Molecular Dynamics Simulations. *ACS Nano* **2013**, *7*, 9428–9442.
- (58) Yin, H.; Slusky, J. S.; Berger, B. W.; Walters, R. S.; Vilaira, G.; Litvinov, R. I.; Lear, J. D.; Caputo, G. A.; Bennett, J. S.; DeGrado, W. F. Computational Design of Peptides That Target Transmembrane Helices. *Science* **2007**, *315*, 1817–1822.
- (59) Najumudeen, A. K.; Kajanajmudeen, A. Receptor Tyrosine Kinase Transmembrane Domain Interactions: Potential Target for “Interceptor” Therapy. *Sci. Signaling* **2010**, *3*, jc6.
- (60) Arpel, A.; Sawma, P.; Spenlé, C.; Fritz, J.; Meyer, L.; Garnier, N.; Velázquez-Quesada, I.; Husseinet, T.; Aci-Sèche, S.; Baumlin, N.; Genest, M.; Brasse, D.; Hubert, P.; Crémel, G.; Orend, G.; Laquerrière, P.; Bagnard, D. Transmembrane Domain Targeting Peptide Antagonizing ErbB2/Neu Inhibits Breast Tumor Growth and Metastasis. *Cell Rep.* **2014**, *8*, 1714–1721.
- (61) Bennasroune, A.; Fickova, M.; Gardin, A.; Dirrig-Grosch, S.; Aunis, D.; Crémel, G.; Hubert, P. Transmembrane Peptides as Inhibitors of ErbB Receptor Signaling. *Mol. Biol. Cell* **2004**, *15*, 3464–3474.
- (62) He, L.; Shobnam, N.; Hristova, K. Specific Inhibition of Pathogenic Receptor Tyrosine Kinase Activation by Its Transmembrane Domain. *Biochim. Biophys. Acta, Biomembr.* **2011**, *1808*, 253–259.
- (63) Zhang, J.; Lazaridis, T. Transmembrane Helix Association Affinity Can Be Modulated by Flanking and Noninterfacial Residues. *Biophys. J.* **2009**, *96*, 4418–4427.